European Polymer Journal 210 (2024) 112989

Contents lists available at ScienceDirect

European Polymer Journal

journal homepage: www.elsevier.com/locate/europolj

Design of cross-linkable polypept(o)ide-based AB_3 miktoarm star polymers through advances in PeptoMiktoStar synthesis

David Schwiertz [a,b], Alina Heck [c], Christian Muhl [a,b], Su Lu [a], Matthias Barz [a,b,*]

[a] BioTherapeutics Division, Leiden Academic Centre for Drug Research (LACDR), Leiden University, Einsteinweg 55, Leiden 2333CC, the Netherlands
[b] Department of Dermatology, University Medical Center, Johannes Gutenberg-University Mainz (JGU), Obere Zahlbacher Straße 63, 55131 Mainz, Germany
[c] Max Planck Institute for Polymer Research, Ackermannweg 10, 55128 Mainz, Germany

ARTICLE INFO

Keywords:
PeptoMiktoStar
Polypept(o)ides
Polysarcosine
Ring-Opening Polymerization

ABSTRACT

Advances in polymer chemistry can provide convenient access to more complex polymeric architectures, such as miktoarm star polymers. In comparison to their linear counterparts, the physical properties of miktoarm star polymers can substantially differ. Their complex synthesis, characterization, and purification, however, makes it a challenging task to prepare well-defined structures with multiple arms of adjustable chemical nature. In this work, well-defined cross-linkable polypept(o)ide-based AB_3 miktoarm star polymers were achieved, taking advantage of a novel asymmetric tetrafunctional initiator system with different orthogonal protecting groups. The first controlled living ring-opening polymerization (ROP) of sarcosine *N*-carboxyanhydride yields a three-armed polysarcosine (pSar) macroinitiator with low molecular weight dispersity ($Đ \sim 1.1$), while a reactive polypeptide arm can be synthesized upon cleavage of the remaining protective group. The established reactive *S*-alkylsulfonyl protecting group bearing polypeptides poly(*S*-ethylsulfonyl-L-cysteine) (pCys(SO_2Et)) and poly(*S*-ethylsulfonyl-L-homocysteine) (pHcy(SO_2Et) were implemented into the asymmetric star architecture. The presence of the well-defined cross-linkable AB_3 PeptoMiktoStars was verified through the characterization via ^{1}H NMR, ^{1}H DOSY, and SEC, revealing structures with dispersity indices of 1.1–1.2 and precise control over the degree of polymerization of each individual polymer chain. In aqueous solution, both types of PeptoMiktoStars form polymeric micelles. The size and morphology can be tuned by secondary structure directed self-assembly: the pHcy(SO_2Et)$_{20}$(pSar$_{100}$)$_3$ polymers form spherical micelles whilst the pCys(SO_2Et)$_{20}$(pSar$_{100}$)$_3$ assembled into worm-like micelles. Therefore, this synthetic methodology provides not only access to well-defined reactive miktoarm star polymers, but also allows for the engineering of polymeric micelles based on PeptoMiktoStars.

1. Introduction

Multiple applications from life sciences to nanotechnology are in high demand for polymers with precisely controlled microstructure and functionality [1]. Despite the fact, that linear polymers have typically dominated in these domains, developments of new synthetic methodologies enabled the realization of more complex polymer structures [2]. As a result, star-shaped polymers, which are branched topologies with at least three linear polymer arms radiating from a central core, have attracted considerable attention [3]. Among star-shaped polymers, miktoarm star polymers, also referred to as heteroarm star polymers, build an interesting subgroup. The miktoarm star polymers possess an asymmetric A_mB_n-architecture and allow the adjustment of polymer density at the hydrophilic/hydrophobic interface in amphiphilic systems, making them most promising in improving the stealth-like nature of polymeric micelles, polyplexes, colloidal or lipid-based nanoparticles in therapy, diagnosis or theragnostic applications. These different polymeric arms can thereby differ in terms of the length, composition, topology, and functionalities [4]. This chemical flexibility allows convenient finetuning of nanoparticle properties, which can hardly be accomplished with the linear counterparts [5–7]. In general, the star-shaped polymers can be realized through the “core-first”, “arm-first” or “coupling onto” approach [8]. To implement the asymmetric topology, multiple protection/deprotection steps, orthogonality, and varied polymerization techniques, are generally required in combination with aforementioned approaches, depending on the specific type of miktoarm

* Corresponding author at: Biotherapeutics Division, Leiden Academic Centre for Drug Research (LACDR), Leiden University, Einsteinweg 55, Leiden 2333CC, The Netherlands.
E-mail address: m.barz@lacdr.leidenuniv.nl (M. Barz).

https://doi.org/10.1016/j.eurpolymj.2024.112989
Received 30 December 2023; Received in revised form 23 March 2024; Accepted 26 March 2024
Available online 27 March 2024

star polymer in need [2], thereof making their controlled synthesis the most challenging tasks in the field of modern polymer science [9].

As one of the numerous synthetic materials available for nanomedicines, polypept(o)ides represent an interesting class of polymers for biomedical applications, since they allow the synthesis of functional polymers based exclusively on endogenous amino acids under controlled living conditions [10]. These hybrid systems combining polypeptoids, e.g., polysarcosine (pSar) or poly(*N*-ethylglycine) (pNEtGly), and multifunctional polypeptides, can be conveniently synthesized by controlled living ring-opening polymerization (ROP) of the corresponding *N*-carboxyanhydrides (NCAs), yielding polymers with narrow molecular weight distributions and high end group fidelity [11,12]. Among them, pSar exists as a random coil structure in aqueous solution and represents exclusively an hydrogen bond acceptor and therefore adheres the Whitesides rules for protein resistant materials [13]. Therefore, pSar is considered a most promising alternative to poly (ethylene glycol) (PEG) in biomedical applications, due to its increased safety profile including a reduced cytokine release [14,15] and improved immunogenicity [16] to overcome PEG-related adverse effects, such as complement activation [17] and the accelerated blood clearance phenomenon induced by antiPEG-antibodies [18,19]. The stealth-like pSar has been successfully blocked with a variety of functional polypeptides, resulting in core–shell structures, that excelled in nanomedicine studies [20–26]. Additionally, we have taken advantage from the realization of linear block copolypept(o)ides to create well-defined symmetrical 3-arm and 6-arm star block copolymers, referred to as PeptoStars, as drug delivery systems or functional carriers for siRNA delivery [27,28]. Moreover, several other research groups have demonstrated the benefits of symmetrical star-shaped polymers based on polypept(o)ides in various applications [29–31].

Importantly, the *in vivo* stability of non-cross-linked polymeric micelles can be limited and disassemble may rapidly occur upon injection, as a result of dilution effect (making the concentration below the critical micelle concentration), followed by the binding of the resulting unimers to the blood components or cells [32,33]. In order to improve the stability of micelles and further prevent their disassembly in the bloodstream, core cross-linking is an established methodology [34]. By introducing the reactive *S*-alkylsulfonyl protecting group to cysteine and homocysteine, our group has established the core cross-linked polymeric micelles by rapid and chemoselective disulfide formation [35–39]. By differentiating between soft and hard nucleophiles, this reactive group permits living amine-initiated ROP of *S*-alkylsulfonyl-protected NCAs. As outlined, the core cross-linking strategy already demonstrated the potential to introduce additional stabilizing factors and control over drug release *in vivo* into linear polypept(o)ide systems [40–42]. In order to synthesize cross-linkable miktoarm stars, we combined a core bearing multiple pSar arms with an arm of either poly(*S*-ethylsulfonyl-L-cysteine (pCys(SO_2Et)) or poly(*S*–ethylsulfonyl-L-homocysteine (pHcy(SO_2Et))). These two differ among reactivity and molecular weight in their secondary structure formation, since pCys(SO_2Et) forms an anti-parallel β-sheet, while pHcy(SO_2Et) adopts an α-helical topology [43]. Until now, these functional groups could not be incorporated into Pepto-MiktoStars, since the *S*-alkylsulfonyl group is not stable under the commonly applied conditions, e.g., basic reactivation of the polypeptide macroinitiator [44]. It is therefore necessary to develop an alternative strategy that allows the integration of sensitive groups into the system in a final step.

In this study, we report such a synthetic approach. Here, a "core-first" method utilizing orthogonal protecting groups, allows the introduction of sensitive functional groups, such as the *S*-alkylsulfonyl protecting group, into the miktoarm star polymers. The synthesis was achieved by an inverse strategy in contrast to the established method [44]. This method provides the ability to combine the aforementioned advantages of the miktoarm star topology with those of core cross-linking by chemoselective disulfide formation, which in addition lays the foundation for the incorporation of additional reactive groups.

2. Experimental section

2.1. Materials and methods

Materials, solvents and chemicals were purchased from Sigma Aldrich and used as received unless stated otherwise. Hexafluoroisopropanol and potassium trifluoroacetate were bought from Fluorochem. *N,N*-Dimethylformamide (99.8 %, extra dry, over molecular sieve) was bought from ACROS ORGANICS and handled under exclusion of light and oxygen. Prior to use as solvent for polymerization reactions, it was purified by multiple freeze–pump–thaw cycles to remove residual amine impurities. Diisopropylethylamine was purified/dried by stirring over potassium hydroxide for three days, subsequential distillation into a pre-dried Schlenk flask equipped with molecular sieves and stored at −20 °C under light and oxygen exclusion. Trifluoracetic acid was purchased from Carl Roth. To monitor NCA polymerization progress, attenuated total reflectance Fourier transformed infrared (ATR-FTIR) spectroscopy was utilized, correlating progress to respective NCA carbonyl bands at 1853 cm^{-1} and 1786 cm^{-1}. Measurements were performed at ambient temperature on a FT/IR-4100 (JASCO) equipped with an ATR sampling accessory (MIRacle TM, Pike Technologies) and spectra were visualized as well as analyzed using Spectra Manager 2.0 software (JASCO). Polymer analytics have been performed by ^{1}H NMR spectroscopy, including Diffusion Ordered Spectroscopy (DOSY) experiments, carried out on a Bruker Avance I (AV-500 MHz) at ambient temperature and a concentration of 15 mg/mL. MestReNova software (version 12.0.2) was used to analyze spectra with calibration by the solvent signal. Deuterated *N,N*-dimethyl sulfoxide as solvent for NMR experiments was purchased from Deutero GmbH. Further, polymers have been analyzed by Size Exclusion Chromatography (SEC), utilizing hexafluoroisopropanol as eluent containing 3 mg/mL potassium trifluoroacetate. Measurements were carried out at 40 °C with a flow rate of 1 mg/mL and calibrated by the toluene signals as internal standard. The column setup (PFG columns with modified silica gel, particle size 7 μm, porosity: 100 Å + 1000 Å) as well as the PSS WinGPC software to monitor and analyze elution diagrams were purchased from PSS Polymer Standard Service GmbH. Millipore water was obtained from a Milli-Q A + system with resistivity of 18.2 MΩ/cm and values for organic carbon of < 5 ppb. Lyophilization to isolate polymers from aqueous solutions was performed on a VirTis BenchTop Pro Freeze Dryer from SP Scientific Products. Electrospray-ionization mass spectrometry (ESI-MS) mass spectra were recorded by an agilent 6545 QTOF-MS (Santa Clara, Ca, USA). Samples were prepared in methanol at 0.1 mg/mL. Transmission electron microscopy (TEM) was performed on a FEI Tecnai G2 Spirit microscope equipped with a Gatan US1000 2 k x 2 k CCD camera an LaB_6 cathode operated at 120 kV. Images were recorded using freshly glow discharged carbon coated copper grids (CF300-Cu, 300 mesh). For negatively stained samples, 5 μL nanoparticle solution (c = 25 mg·L^{-1}) was drop-coated on the TEM grid, removed with a filter paper after 1 m. Afterwards 5 μL uranyl acetate solution (2 wt% in ethanol) was added and removed after 15 s incubation time. All sample-deposited grids were air-dried overnight before measurements. Software ImageJ 1.52 h (National Institutes of Health, USA) was used for image evaluation.

2.2. Synthesis

Full synthetic procedures, including initiator and polymer synthesis, particle preparation, purification and characterization data are provided in the Supporting Information.

3. Results and discussion

3.1. Development of tetrafunctional initiators

In order to establish a synthetic pathway for cross-linkable AB_3

PeptoMiktoStars, the current strategy had to be further refined [44]. The confirmed method utilized a "core-first" approach with a tetrafunctional initiator (**C1** in Fig. 1) bearing a carboxybenzyl (Cbz) and three *tert*-butyloxycarbonyl (Boc) groups to enable implementation of the orthogonal protecting group strategy. The corresponding linear polypeptide macro-.

initiators were first synthesized and then subjected to several end-group modifications (acetylation of the first initiating site, Boc-deprotection and basic reactivation of the amine functionalities). Finally, these macroinitiators become well-defined AB_3 miktoarm stars following simultaneous ROP of Sar-NCA at three initiating sites. The labile *S*-alkylsulfonyl protecting group, does not remain intact throughout the multistep synthesis. Therefore, we developed an alternative strategy that may enable the implementation of susceptible functionalities. Scheme 1 illustrates the approach chosen for this purpose.

Contrary to the primary method, this methodology starts with the synthesis of a 3-arm macroinitiator, from which the *S*-alkylsulfonyl-cysteine or -homocysteine arm is synthesized in the final polymerization step (see Scheme 1). In light of these changes, the tetrafunctional initiator must be optimized. A complete overview of the comprehensive initiator development process with all intermediate steps can be seen in **Fig. S4**, and the most promising representatives are summarized in Fig. 1. In this context, the initiator **C1** represents the tetrafunctional core that was already successfully utilized in the realization of classic AB_3 PeptoMiktoStars and thus serves as the foundation for further developments. All tetrafunctional initiators could be obtained in a high degree of purity, as indicated by ^{1}H NMR (**Figs. S5–S17**). The initiators' purity is crucial for the subsequent controlled living ROP of NCAs to achieve well-defined structures. The impurities may act as chain-transfer agents, terminate growing species, or initiate themselves, resulting in linear homo polymer contaminants, which can be hardly removed from the final miktoarm star polymer. Following deprotection, **C1** was initially used in the inverse approach after Boc-deprotection until the successful synthesis of the three-armed pSar macroinitiator (**Figs. S25 and S30**).

Unluckily, the carboxybenzyl (Cbz) deprotection was not successfully executed at the macroinitiator level (**Fig. S31**), making the failure of this approach. The successful synthesis of initiators **C2** and **C3** has been achieved up to the stage of the macroinitiator analogous to **C1**. In both cases, well-defined three-armed cores could be obtained with narrow molecular weight distributions.($Đ = 1.1$) and high control over the pSar chain lengths (**Figs. S26, S27, S30**). Moreover, neither **C2** nor **C3** suffered from the same problem as the Cbz-protected **C1** core, since deprotection of both protecting groups (Fmoc and TFA) could be accomplished after formation of the corresponding macroinitiators. Unfortunately, in the final step neither of these two systems led to the desired well-defined miktoarm star architecture, as it is evident from the SEC curves that either linear polymers were formed from impurities or the integrity of the macroinitiator was impaired during deprotection (**Fig. S31**). In the course of further research, the **C4** initiator was finally developed, which has the protective groups in vice versa arrangement compared to the **C1** initiator. As part of a 6-step process, the **C4** initiator was derived analogously to the other multifunctional cores from tris (hydroxymethyl)-aminomethane (TRIS) as starting material (Fig. 2). To minimize the risk of site reactions during NCA polymerizations, impurities were removed by column chromatography after each synthetic step. The chemical identity and purity of all intermediate products was confirmed by ^{1}H NMR (**Figs. S15–S17**) and the purity of the final **C4** core was additionally analyzed via ESI mass spectrometry (**Fig. S18**).

3.2. Core Cross-Linkable PeptoMiktoStars

To use **C4** in the macroinitiator synthesis, the related amine functionalities need to be deprotected. Cleavage of the Cbz-protecting groups was achieved under reductive conditions using methanol and palladium in a hydrogen atmosphere, verified via ^{1}H NMR (**Fig. S23**) and led to a trifunctional initiator with equally reactive initiation sites enabling simultaneous chain growth. The **C4** core obtained in this manner was subsequently used for the preparation of the three-arm macroinitiator by utilization in a controlled living ROP with Sar-NCA. As this chain length has been established for non-cross-linkable PeptoMiktoStars, a degree of polymerization (DP_n) of 300 (3 x 100) was chosen for pSar [44]. In accordance with the analytical results, the chain length could be controlled precisely by the monomer-to-initiator feed ratio. From the ^{1}H NMR spectra, the DP_n can be determined by relating the signals of the *tert*–butyloxycarbonyl (Boc) protecting group and the aminohexyl-spacer (Ahx) with the signals of the back-bone protons of pSar. Polymerizations were conducted in absolute DMF at 0 °C (less than 50 ppm water) and the monomer conversion was tracked in IR spectroscopy by disappearance of the NCA vibration bands at 1853 and 1786 cm^{-1}. Utilizing azide-containing capping agents, terminal functionalities can be introduced to the resulting macroinitiator during a quenching step after complete monomer conversion. As a result of the quantitative azide functionalization implemented in this manner, it is possible to benefit from the well-established strain-promoted-azide-alkyne cycloaddition

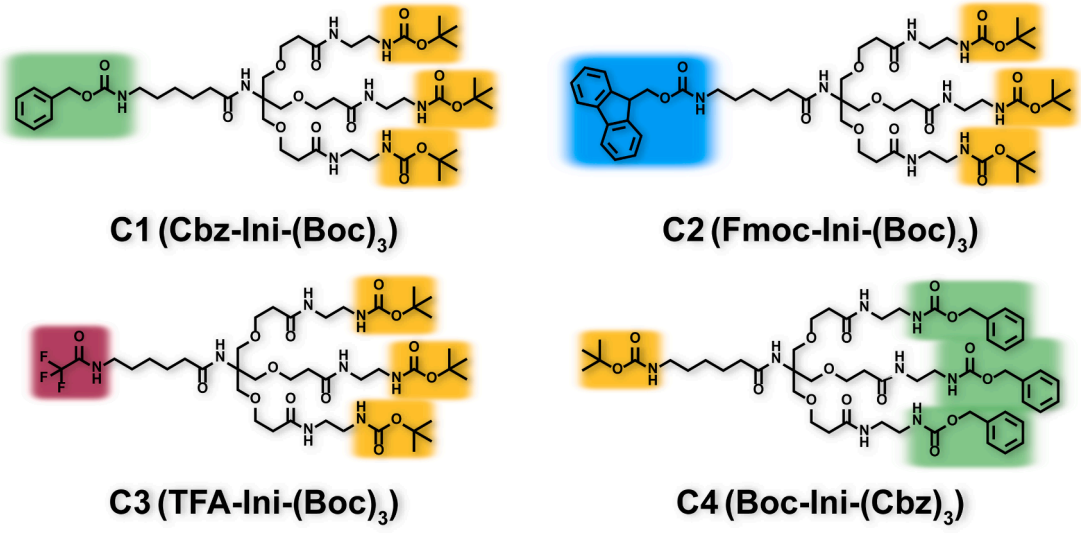

Fig. 1. Most promising representatives from the tetrafunctional initiator development.

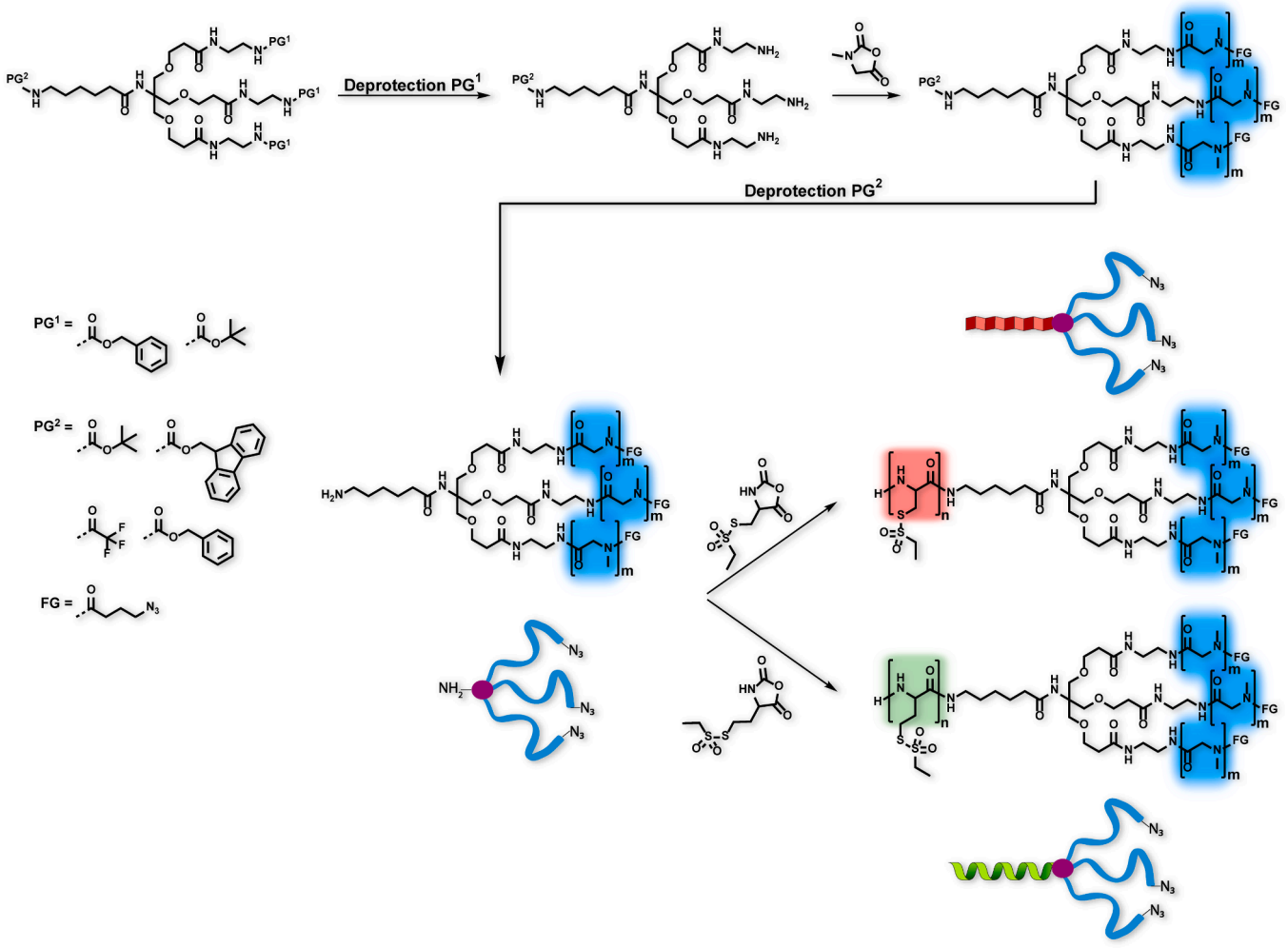

Scheme 1. Strategy exemplified for the inverse approach facilitating core cross-linkable AB_3 PeptoMiktoStars.

(SPAAC) by introducing e.g. targeting structures with a high selectivity under mild reaction conditions [20,37,45]. Afterwards, the pSar-based **C4** macroinitiator was precipitated in cold diethyl ether and analyzed by ^{1}H NMR and SEC in hexafluoroisopropanol (HFIP) (Fig. 4). Analytical data is summarized in Table 1. The three-arm **C4** macroinitiator exhibits a monomodal molecular weight distribution with a low dispersity of $Đ =$ 1.1, thus revealing simultaneous initiation and uniform chain growth. It is noteworthy, that the use of the different initiators (**C1-C4**) had in general no significant influence on the molecular weight distribution determined by SEC of the respective three-arm pSar cores. As demonstrated in **Fig. S30**, the various macroinitiators result in almost

identical SEC elugrams indicating that initiator effects are absent, and the polymerization proceeds under well controlled conditions and enables precise adjustments of the resulting molecular weights. As confirmed by ^{1}H-DOSY NMR, there is only one diffusing species containing all pSar and initiator signals with the same diffusion coefficients for all macroinitiators, which underlines the absence of linear homo polymers caused by impurities in the initiator, solvents, or the occurrence of chain transfer reactions (**Fig. S29**) [38]. Upon confirmation of the successful macroinitiator synthesis, the Boc-protecting group was quantitatively removed in a 1:1 mixture of H_2O/TFA at rt. Liberation of the amine functionality was verified by disappearance of the characteristic Boc signal at 1.3–1.5 ppm (**Fig. S33**). Following purification by dialysis against saturated sodium hydrogen carbonate solution and MilliQ water, it was verified via HFIP SEC that the three-arm macroinitiator retained its integrity and is thus suitable for the synthesis of the thiol-reactive PeptoMiktoStars (**Fig. S34**).

In the next step, the three-arm macroinitiator was applied in the synthesis of the poly(*S*-ethylsulfonyl-L-cysteine (pCys(SO_2Et)) and poly (*S*–ethyl-sulfonyl-L-homocysteine (pHcy(SO_2Et)) arms. The polymerization was carried out in the same manner as the macroinitiator synthesis, but at −10 °C, in order to preserve the functionality of the *S*-alkylsulfonyl groups during amine-initiated NCA polymerization and to increase the quality of the respective analytical data [39,46]. Characterization of the final AB_3 PeptoMiktoStars was performed by ^{1}H NMR, ^{1}H DOSY and SEC in HFIP as summarized in Figs. 3 and 4. As expected for the ROP of NCAs, the ratio of monomer to macroinitiator is sufficient to precisely control the DP_n for the two different hydrophobic polypeptide arms introduced. Arm lengths were determined via ^{1}H NMR by relating the isolated signal of the α-proton at 4.68 ppm for pCys(SO_2Et) and the amide proton at 8.32 ppm for pHcy(SO_2Et), respectively, underlining that the desired DP_n of 20 has been achieved. SEC analyses further reveals a clear shift in the elution volume maxima from higher to lower elution times and therefore, indicates successful chain extension and PeptoMiktoStars with narrow size distributions and low dispersities of $Đ = 1.2$ for both systems. The slight broadening of polymer elugrams is -in all probability- caused by the secondary structure formation of the polypeptide arm, which influences the hydrodynamic volume of polypeptides [47,48]. The successful and highly controlled synthesis of AB_3 miktoarm star polymers in the absence of linear homopolymer or symmetrical homoarm star polymer impurities were confirmed by SEC and ^{1}H DOSY NMR spectroscopy. Further, the presence of only one polymeric species and alignment of all polymer and initiator signals confirms the structural integrity of the final reactive PeptoMiktoStar polymers.

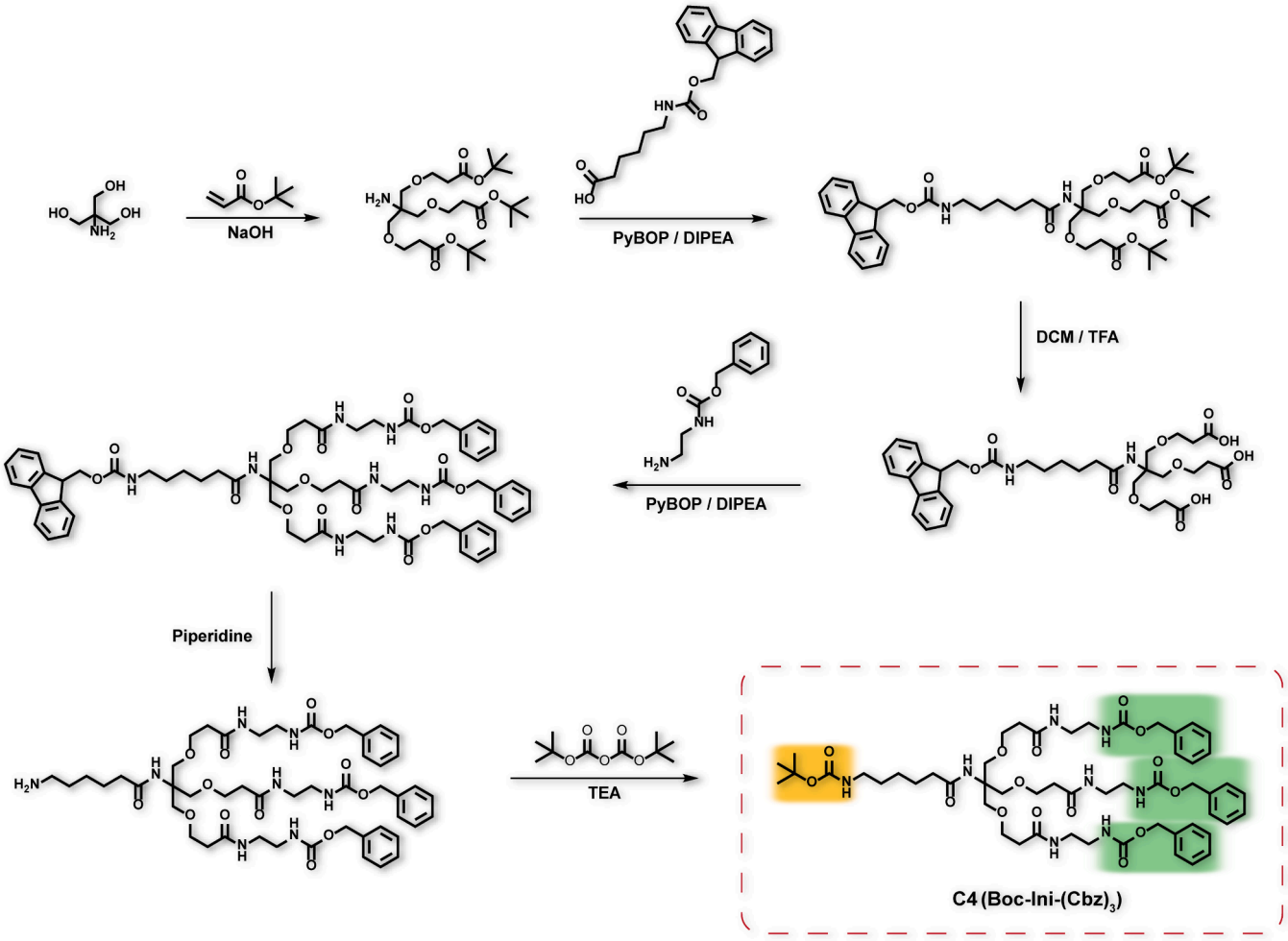

Fig. 2. Synthetic pathway of the auspicious **C4** initiator for the realization of cross-linkable AB_3 PeptoMiktoStars.

Table 1
Analytical data of the different cross-linkable AB_3 PeptoMiktoStars synthesized.

Polymer	DP_n [a] (calc.)	DP_n [b] (found)	M_n [c] / g·mol^{-1}	$Đ$ [d]
pCys(SO_2Et)$_{20}$(pSar$_{100}$-N_3)$_3$	20/(1 0 0)$_3$	20/(1 0 0)$_3$	25,200	1.2
pHcy(SO_2Et)$_{20}$(pSar$_{100}$-N_3)$_3$	20/(1 0 0)$_3$	20/(1 0 0)$_3$	25,500	1.2

[a] Calculated degree of polymerization using DP_n = [M]/[I]. [b]Determined by 1H NMR in DMSO-d_6. [c]Determined by obtained chain lengths from ^{1}H NMR after subtraction of the corresponding initiator's molecular weight. [d]Determined by SEC in HFIP using PMMA standards.

These results demonstrate that the controlled nature of the polymerization of both used NCAs is also preserved by the utilization of the three-arm macroinitiators. Consequently, the outlined synthetic approach enables the integration of reactive polypeptides into the AB_3 architecture of PeptoMiktoStars, which enables their use for bio reversible cross-linking in polymeric micelles or polyplexes.

3.3. Solution Self-Assembly

The self-assembly of the two obtained AB_3 miktoarm star polymers was conducted using the established solvent switch method and the resulting nanoparticles were investigated in terms of size and shape in relation to their linear analogues [36]. To obtain the thermodynamically favored micelles, the PeptoMiktoStars were first dissolved in a good solvent (*N,N*–dimethylacetamide), followed by aggregation in the presence of 20 vol% 1 mM acetate buffer and subsequently dialyzed against 1 mM acetate buffer (over 24 h). Once the solvent exchange process was finished, the micelles underwent core cross-linking by introducing 1,6-hexanedithiol through chemoselective disulfide formation, which preserves the fixed morphology obtained by the aspired secondary structure-directed self-assembly [42,49].

The morphologies of the self-assembled structures were revealed by transmission electron microscopy (TEM) and the encoded secondary structures were validated by FTIR. As dictated by the TEM images in Fig. 5, the homocysteine based miktoarm star polymers formed spherical micelles with diameter of ~ 40 nm, whilst the cysteine-based equivalents underwent the secondary structure directed self-assembly and formed worm-like micelles, with a similar diameter of ~ 40 nm and an average length of around 150 nm [36,43]. In contrast to their linear counterparts [36,42,49] the resulting worm-like micelles are shorter, with better flexibility and less rigidity, that can be attributed to the increased steric demand of the miktoarm architecture, which might further result in a less compact packing of cysteine blocks.

The secondary structures in both miktoarm star polymers were characterized by FTIR in the solid state (**Fig. S36**) [43,47,50]. The predominant signals of the amide bands at 1547 and 1315 cm^{-1} (Amide II, Amide III) revealed the α-helical structure of the pHcy(SO_2Et) arm, despite the Amide I peak's overlap with the random coil structure of pSar (1650 cm^{-1}). The shoulder at 1703 cm^{-1} indicates the antiparallel alignment of the β-sheets, which is attributed to the pCys(SO_2Et)-arm. Altogether, the high control achieved in the synthesis of PeptoMiktoStars enables secondary structure-directed self-assembly as well as core cross-linking and functionalization, which provides access to a new

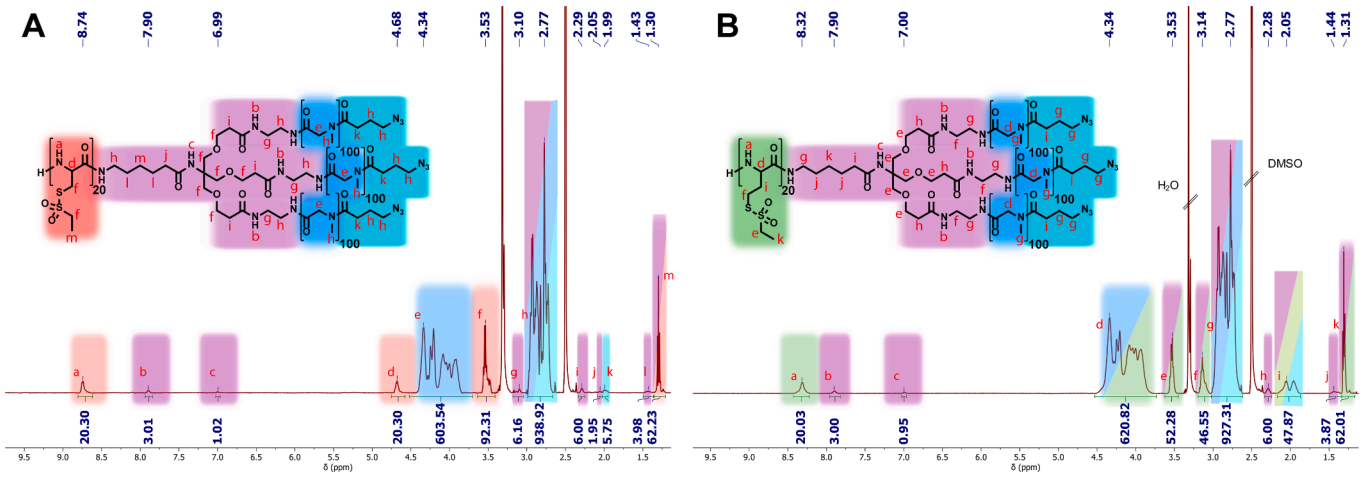

Fig. 3. ^{1}H NMR analysis of cross-linkable AB_3 PeptoMiktoStars with variations in the *S*-alkylsulfonyl protecting group bearing section in DMSO-d_6. (A) ^{1}H NMR spectrum of $pCys(SO_2Et)_{20}(pSar_{100}\text{-}N_3)_3$. (B) ^{1}H NMR spectrum of $pHcy(SO_2Et)_{20}(pSar_{100}\text{-}N_3)_3$.

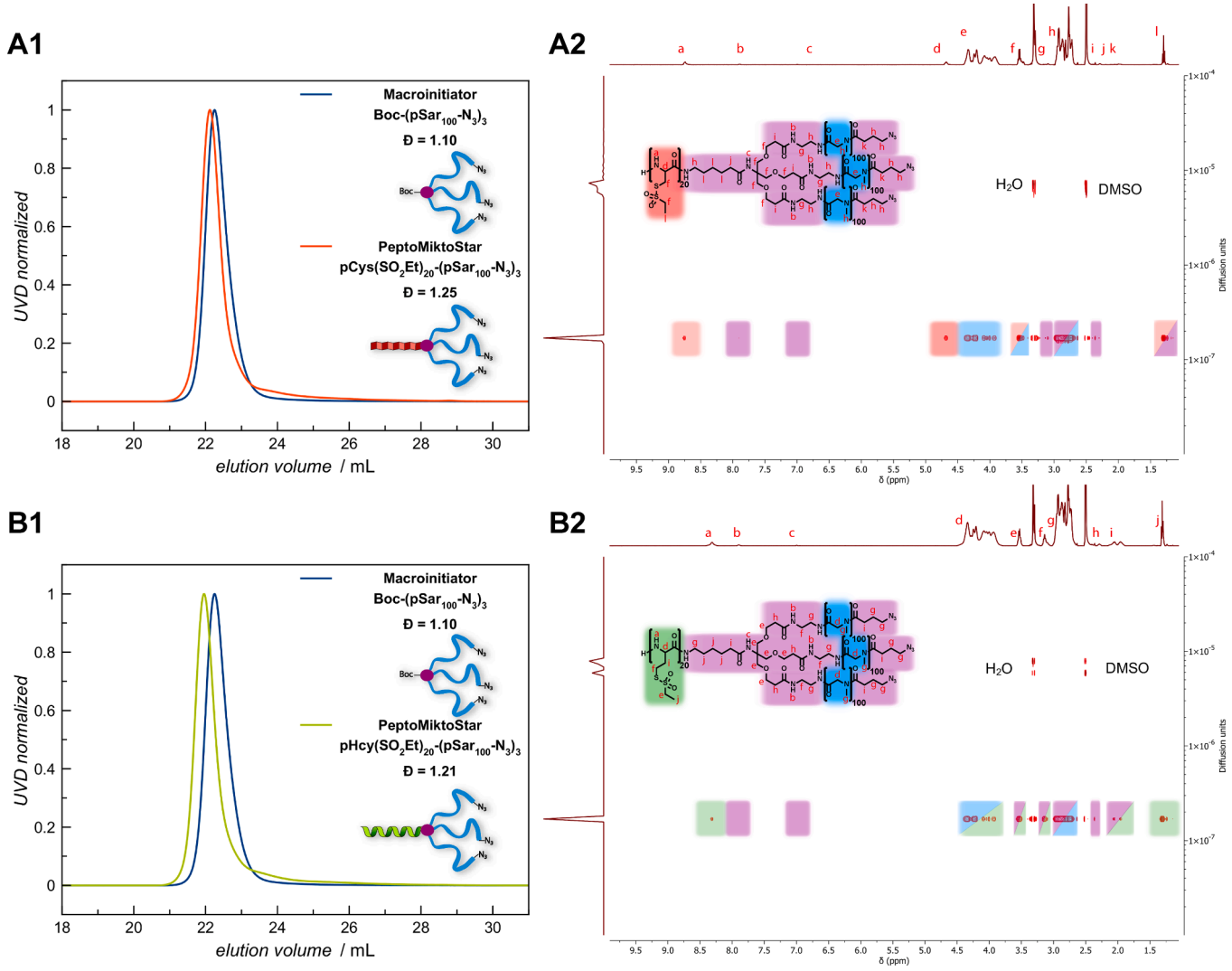

Fig. 4. Analyses of the cross-linkable AB_3 PeptoMiktoStars obtained from the investigated inverse approach with variations regarding the functional arm. (A) Characterization of the cysteine-based PeptoMiktoStar. (A1) HFIP SEC traces of $pCys(SO_2Et)_{20}\text{-}(pSar_{100}\text{-}N_3)_3$. (A2) ^{1}H DOSY NMR of $pCys(SO_2Et)_{20}(pSar_{100}\text{-}N_3)_3$. (B) Characterization of the homocysteine-based PeptoMiktoStar. (B1) HFIP SEC traces of $pHcy(SO_2Et)_{20}(pSar_{100}\text{-}N_3)_3$. (B2) ^{1}H DOSY NMR of $pHcy(SO_2Et)_{20}(\text{-}pSar_{100}\text{-}N_3)_3$.

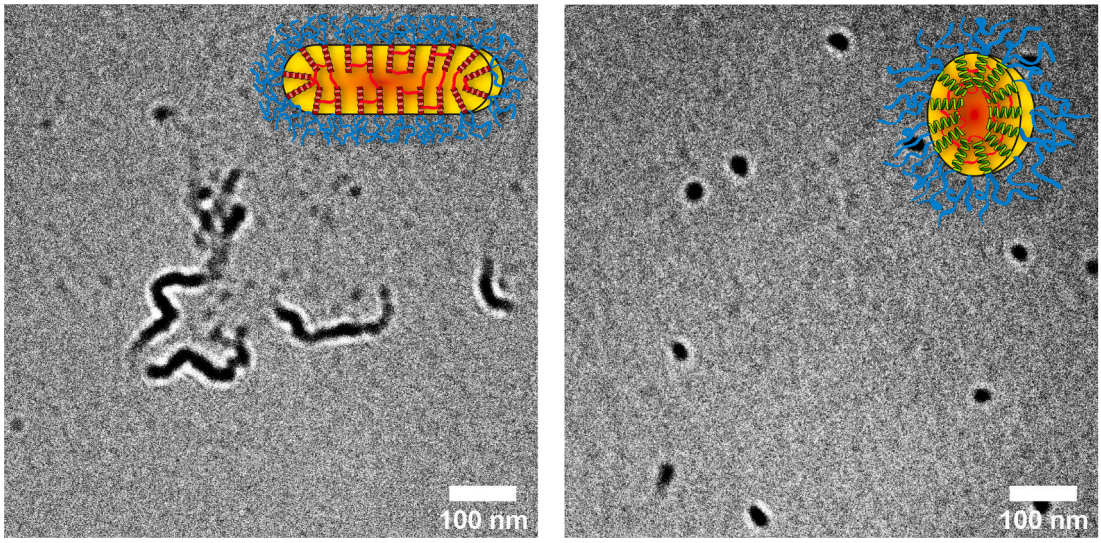

Fig. 5. TEM images of worm-like micelles based on pCys$(SO_2Et)_{20}(pSar_{100})_3$ (left), and spherical micelles based on pHcy$(SO_2Et)_{20}(pSar_{100})_3$. (right). Scale bar = 100 nm.

generation of core cross-linked PeptoMicelles.

4. Conclusion

To conclude, we developed a novel synthetic approach to successfully realize core cross-linkable micelles consisting of PeptoMiktoStars, miktoarm star polymers combining polypeptoids and polypeptides in a single polymer. Through the design of multiple tetrafunctional initiator systems and associated versatile orthogonal protecting group strategies, it is finally possible to advance to macroinitiator systems, which enabled the introduction of functional components as the *S*-alkylsulfonyl protected cysteine and homocysteine into the miktoarm architecture. This approach enables access to well-defined AB_3 polypept(o)ide-based miktoarm star polymers with narrow molecular weight distributions, low dispersity indices of 1.1–1.2 and precise control over the resulting lengths of the individual arms. Depending on the choice of monomer, the morphology of the resulting micelles can be controlled by secondary structured self-assembly in aqueous solution. The overall behavior is comparable to linear polypept(o)ide block copolymers, but the enhanced bulkiness at the hydrophilic hydrophobic interphase in amphiphilic AB_3 miktoarm star polymers reduces the rigidity of pCys(SO_2Et) based worm-like micelles. In contrast, core cross-linking can be performed as efficiently as for the linear block copolypept(o)ides. Therefore, the presented strategy enables the combination of the advantages of miktoarm star polymers with those of the linear counterparts, namely morphology control and providing a framework for future drug delivery designs.

CRediT authorship contribution statement

David Schwiertz: Writing – original draft, Visualization, Investigation, Formal analysis, Data curation. **Alina Heck:** Data curation. **Christian Muhl:** Methodology, Data curation. **Su Lu:** . **Matthias Barz:** Writing – review & editing, Validation, Supervision, Resources, Project administration, Investigation, Funding acquisition, Conceptualization.

Declaration of competing interest

The authors declare the following financial interests/personal relationships which may be considered as potential competing interests: Matthias Barz reports financial support was provided by German Research Foundation. Matthias Barz reports a relationship with Curapath that includes: consulting or advisory. Matthias Barz is co-inventor of the patent "Thiol-protected amino acid derivatives and uses thereof" and receives royalties . The other authors declare that they have no known competing financial interests or personal relationships that could have appeared to influence the work reported in this paper.

Data availability

Data will be made available on request.

Acknowledgement

M.B. would like to acknowledge financial support by the German Research Foundation (DFG) within the Collaborative Research Centres SFB1066-3 Project B12 and B5.

Appendix A. Supplementary data

Supplementary data to this article can be found online at https://doi.org/10.1016/j.eurpolymj.2024.112989.

References

[1] M. Liu, J.R. Blankenship, A.E. Levi, Q. Fu, Z.M. Hudson, C.M. Bates, Chem. Mater. 34 (14) (2022) 6188–6209.
[2] K. Khanna, S. Varshney, A. Kakkar, Polym. Chem. 1 (2010) 1171–1185.
[3] W. Wu, W. Wang, J. Li, Prog. Polym. Sci. 46 (2015) 55–85.
[4] J. Ren, T.G. McKenzie, Q. Fu, E.H.H. Wong, J. Xu, Z. An, S. Shanmugam, T.P. Davis, C. Boyer, G.G. Qiao, Chem. Rev. 116 (12) (2016) 6743–6836.
[5] V. Lotocki, H. Yazdani, Q. Zhang, E.R. Gran, A. Nyrko, D. Maysinger, A. Kakkar, Macromol. Biosci. 21 (2) (2021) 1–13.
[6] Z. Ma, S.W. Wong, H. Forgham, L. Esser, M. Lai, M.N. Leiske, K. Kempe, G. Sharbeen, J. Youkhana, F. Mansfeld, J.F. Quinn, P.A. Phillips, T.P. Davis, M. Kavallaris, J.A. McCarroll, Biomaterials 2022 (November 2021) 285.
[7] M. Baghbanbashi, H.W. Yong, I. Zhang, V. Lotocki, Z. Yuan, G. Pazuki, D. Maysinger, A. Kakkar, Macromol. Biosci. 22 (10) (2022) 1–14.
[8] M.A. Reith, I. De Franceschi, M. Soete, N. Badi, R. Aksakal, F.E. Du Prez, J. Am. Chem. Soc. 144 (16) (2022) 7236–7244.
[9] A.E. Levi, L. Fu, J. Lequieu, J.D. Horne, J. Blankenship, S. Mukherjee, T. Zhang, G. H. Fredrickson, W.R. Gutekunst, C.M. Bates, Macromolecules 53 (2) (2020) 702–710.
[10] K. Klinker, M. Barz, Macromol. Rapid Commun. 36 (2015) 1943–1957.
[11] P. Heller, A. Birke, D. Huesmann, B. Weber, K. Fischer, A. Reske-kunz, M. Bros, M. Barz, Macromol. Biosci. 14 (2014) 1380–1395.
[12] A. Birke, D. Huesmann, A. Kelsch, M. Weilba, J. Xie, M. Bros, T. Bopp, C. Becker, K. Landfester, M. Barz, Biomacromolecules 15 (2) (2014) 548–557.
[13] E. Ostuni, R.G. Chapman, R.E. Holmlin, S. Takayama, G.M. Whitesides, Langmuir 17 (9) (2001) 5605–5620.

[14] S.S. Nogueira, A. Schlegel, K. Maxeiner, B. Weber, M. Barz, M.A. Schroer, C. E. Blanchet, D.I. Svergun, S. Ramishetti, D. Peer, P. Langguth, U. Sahin, H. Haas, ACS appl, Nano Mater. 3 (11) (2020) 10634–10645.
[15] S. Bleher, J. Buck, C. Muhl, S. Sieber, S. Barnert, D. Witzigmann, J. Huwyler, M. Barz, R. Süss, Small 15 (2019) 50.
[16] P.H. Maurer, D. Subrahmanyam, E. Katchalski, E.R. Blout, J. Exp. Med. 121 (1965) 339–349.
[17] I. Hamad, A.C. Hunter, J. Szebeni, S.M. Moghimi, Mol. Immunol. 46 (2008) 225–232.
[18] K. Son, M. Ueda, K. Taguchi, T. Maruyama, S. Takeoka, Y. Ito, J. Control. Release 322 (2020) 209–216.
[19] L. Hong, Z. Wang, X. Wei, J. Shi, C. Li, J. Pharmacol. Toxicol. Methods 102 (2020) 106678.
[20] C. Kappel, C. Seidl, C. Medina-Montano, M. Schinnerer, I. Alberg, C. Leps, J. Sohl, A.K. Hartmann, M. Fichter, M. Kuske, J. Schunke, G. Kuhn, I. Tubbe, D. Paßlick, D. Hobernik, R. Bent, K. Haas, E. Montermann, K. Walzer, M. Diken, M. Schmidt, R. Zentel, L. Nuhn, H. Schild, S. Tenzer, V. Mailänder, M. Barz, M. Bros, S. Grabbe, ACS Nano 15 (9) (2021) 15191–15209.
[21] N.-J.-K. Dal, G. Schäfer, A.M. Thompson, S. Schmitt, N. Redinger, K.J. Noelia Alonso-Rodriguez, J. Ojong, J. Wohlmann, A. Best, K. Koynov, R. Zentel, U. E. Schaible, G. Griffiths, M. Barz, F.J. Fenaroli, Control, Release 354 (January) (2023) 851–868.
[22] K. Johann, T. Bohn, F. Shahneh, N. Luther, A. Birke, H. Jaurich, M. Helm, M. Klein, V.K. Raker, T. Bopp, M. Barz, C. Becker, Nat. Commun. 12 (1) (2021) 1–9.
[23] T.A. Bauer, N.K. Horvat, O. Marques, S. Chocarro, C. Mertens, S. Colucci, S. Schmitt, L.M. Carella, S. Morsbach, K. Koynov, F. Fenaroli, P. Blümler, M. Jung, R. Sotillo, M.W. Hentze, M.U. Muckenthaler, M. Barz, Adv. Healthc. Mater. 10 (2021) 2100385.
[24] D. Bi, D.M. Unthan, L. Hu, J. Bussmann, K. Remaut, M. Barz, H.J. Zhang, Control, Release 356 (January) (2023) 1–13.
[25] C. Lebleu, L. Plet, F. Moussy, G. Gitton, R. Da Costa Moreira, L. Guduff, B. Burlot, R. Godiveau, A. Merry, S. Lecommandoux, G. Errasti, C. Philippe, T. Delacroix, R. Chakrabarti, Int. J. Pharm. 631 (2023) 122501.
[26] B. Mahi, M. Gauthier, N. Hadjichristidis, Biomacromolecules 23 (6) (2022) 2441–2458.
[27] M. Darguzyte, R. Holm, J. Baier, N. Drude, J. Schultze, K. Koynov, D. Schwiertz, S. M. Dadfar, T. Lammers, M. Barz, F. Kiessling, Bioconjug. Chem. 31 (12) (2020) 2691–2696.
[28] R. Holm, D. Schwiertz, B. Weber, J. Schultze, J. Kuhn, K. Koynov, U. Lächelt, M. Barz, Macromol. Biosci. 20 (1) (2020) 1–17.
[29] R.M. England, J.I. Moss, A. Gunnarsson, J.S. Parker, M.B. Ashford, Biomacromolecules 21 (8) (2020) 3332–3341.
[30] D. Skoulas, V. Stuettgen, R. Gaul, S.A. Cryan, D.J. Brayden, A. Heise, Biomacromolecules 21 (6) (2020) 2455–2462.
[31] D. Skoulas, S. Fattah, D. Wang, S.A. Cryan, A. Heise, Macromol. Biosci. 22 (8) (2022) 1–9.
[32] M. Talelli, M. Barz, R.J.F. Rijcken, F. Kiessling, W.E. Hennink, T. Lammers, Nano Today 10 (2015) 93–117.
[33] Y. Shi, T. Lammers, G. Storm, W.E. Hennink, Macromol. Biosci. 17 (1600160) (2017) 1–11.
[34] H.W. Yong, A. Kakkar, Macromol. Biosci. 21 (8) (2021) 2100105.
[35] O. Schäfer, M. Barz, Chem. Eur. J. 24 (2018) 12131–12142.
[36] K. Klinker, O. Schäfer, D. Huesmann, T. Bauer, L. Capeloa, L. Braun, N. Stergiou, M. Schinnerer, A. Dirisala, K. Miyata, K. Osada, H. Cabral, K. Kataoka, M. Barz, Angew. Chem. Int. Ed. 56 (2017) 9608–9613.
[37] O. Schäfer, K. Klinker, L. Braun, D. Huesmann, J. Schultze, K. Koynov, M. Barz, ACS Macro Lett. 6 (2017) 1140–1145.
[38] O. Schäfer, D. Huesmann, C. Muhl, M. Barz, Chem. Eur. J. 22 (2016) 18085–18091.
[39] C. Muhl, O. Schäfer, T. Bauer, H.J. Räder, M. Barz, Macromolecules 51 (20) (2018) 8188–8196.
[40] T.A. Bauer, J. Eckrich, N. Wiesmann, F. Kuczelinis, W. Sun, X. Zeng, B. Weber, S. Wu, N.H. Bings, M.B. Sebastian Strieth, J. Mater. Chem. B. 9 (2021) 8211–8223.
[41] L. Capelöa, M. Yazdi, H. Zhang, X. Chen, Y. Nie, E. Wagner, U. Lächelt, M. Barz, Macromol. Rapid Commun. 43 (12) (2022) 1–9.
[42] T.A. Bauer, J. Schramm, F. Fenaroli, S. Siemer, C.I. Seidl, C. Rosenauer, R. Bleul, R. H. Stauber, K. Koynov, M. Maskos, M. Barz, Adv. Mater. 35 (2023) 2210704.
[43] T.A. Bauer, J. Imschweiler, C. Muhl, B. Weber, M. Barz, Biomacromolecules 22 (5) (2021) 2171–2180.
[44] D. Schwiertz, R. Holm, M. Barz, Polym. J. 52 (1) (2020) 119–132.
[45] G. Yi, J. Son, J. Yoo, C. Park, H. Koo, Biomater. Res. 22 (1) (2018) 1–8.
[46] O. Schäfer, D. Huesmann, M. Barz, Macromolecules 49 (21) (2016) 8146–8153.
[47] D. Huesmann, A. Birke, K. Klinker, S. Türk, H.J. Räder, M. Barz, Macromolecules 47 (3) (2014) 928–936.
[48] T.A. Bauer, C. Muhl, D. Schollmeyer, M. Barz, Macromol. Rapid Commun. 42 (2021) 2000470.
[49] T.A. Bauer, I. Alberg, L.A. Zengerling, P. Besenius, K. Koynov, B. Slu, R. Zentel, I. Que, H. Zhang, M. Barz, Biomacromolecules 24 (8) (2023) 3545–3556.
[50] J.T. Pelton, L.R. McLean, Anal. Biochem. 277 (2) (2000) 167–176.